

Sensorless Control Method in IPMSM Position Sensor Fault for HEV

Sung-Joo Kim*, Yong-Kyun Lee**, Ju-Suk Lee***, Kwang-Woon Lee§, Taesuk Kwon§§ and Hyungsoo Mok†

Abstract – The widely used motors in HEV(Hybrid Electric Vehicles) are IPMSM(Interior Permanent Magnet Synchronous Motor) which has no rotor heat, higher efficiency and advantageous in volume and weight comparing with other motors. For vector control of IPMSM, position information of rotor is required but Resolver is mainly used as the detecting sensor. However, the use of position sensors will reduce the system reliability of hybrid electric vehicles. In this paper, a way to control the motor by sensorless was proposed at the event of sensor failure. We also implemented IPMSM sensorless operation by the expanded EMF(Electro Motive Force) voltage way and harmonic voltage which is applying in the low speed area. And we proposed how to change with sensorless control by detecting the position sensors failure and verified it through experiments.

Keywords: IPMSM, Sensorless control, Position sensor fault

1. Introduction

Recently, research and development across the industries for eco-friendly system has been accelerated by the problems such as air pollution, high oil prices. Of which the automotive industries that have lot of spending fossil fuels, the need for the development of environmentally friendly cars is increasing dramatically. These eco-friendly cars as hybrid electric vehicles and electric vehicle development and production are underway. [5] The widely used motors in HEV(Hybrid Electric Vehicles) are IPMSM (Interior Permanent Magnet Synchronous Motor) which has no rotor heat, higher efficiency and advantageous in volume and weight comparing with other motors. For vector control of IPMSM, position information of rotor is required but Resolver is mainly used as the detecting sensor. As a matter of safety in case of automobiles, how to control the motor without the sensor has been studied when some fault occurs of Resolver Sensors. In this paper, we proposed how to change with sensorless control by applying the extended EMF model, in case the position information sensor go down. In that case using the extended electromotive voltage model the position estimation is not correct owing to small Back-EMF at the extremely low speed and zero speed zone. To complement these points we proposed a way that can estimate the

position with relatively simple way applying harmonic voltage to the D axis voltage. The proposed method is also verified by experiments.

2. Extended EMF Model Sensorless control

As the IPM is modeled by the rotary coordinate which is synchronized with rotating speed, we can get the following Eq. (1).

$$\begin{bmatrix} v_d \\ v_q \end{bmatrix} = \begin{bmatrix} R + pL_d & -\omega_r L_q \\ \omega_r L_d & R + pL_q \end{bmatrix} \begin{bmatrix} i_d \\ i_q \end{bmatrix} + \omega_r K_E \begin{bmatrix} 0 \\ 1 \end{bmatrix} \quad (1)$$

At the above equation, R, L_d , L_q , K_E are wire wound resistance, d axis inductance, q axis inductance, electromotive coefficient respectively, ω_r is rotor speed, V_d and i_d are voltage and current for d axis, V_q and i_q are voltage and current for q axis. Eq. (1) can be simplified as below. [1]

$$\begin{bmatrix} v_d \\ v_q \end{bmatrix} = \begin{bmatrix} R + pL_d & -\omega_r L_q \\ \omega_r L_q & R + pL_d \end{bmatrix} \begin{bmatrix} i_d \\ i_q \end{bmatrix} + \begin{bmatrix} e_{xd} \\ e_{xq} \end{bmatrix} \quad (2)$$

$$\begin{bmatrix} e_{xd} \\ e_{xq} \end{bmatrix} = \begin{bmatrix} 0 \\ (L_d - L_q)(\omega_r i_d - p i_q) + \omega_r K_E \end{bmatrix} = \begin{bmatrix} 0 \\ E_x \end{bmatrix}$$

E_x of above is called extended electromotive voltage. [2] Exact control of IPMSM is possible making control system with Eq. (1) on the condition that knows the exact location of rotor through position sensor. However, there is no way to know exact position without position sensor. Assuming that the estimated axis of the controller is γ - δ , Fig. 1 shows the relation between real d-q and γ - δ . α - β axis is for the fixed coordinate system, and d-q is the rotary coordinate

† Corresponding Author: Dept. of Electrical and Electronic Engineering, Konkuk University, Korea. (hsmok@konkuk.ac.kr)

* Dept. of Electrical and Electronic Engineering, Konkuk University, Korea. (ksj0108@konkuk.ac.kr)

** Technical Research Institute, VCTech Co.,Ltd, Korea. (ykleee@vctech.co.kr)

*** Dept. of Mechanical Air-Conditioning, Gyeonggi College of Science and Technology, Korea. (jslee@gtec.ac.kr)

§ Dept. of Electronic Eng., Mokpo National Maritime University, Mokpo, Korea. (kwlee89@mmu.ac.kr)

§§ R&D Institute, Hyundai Mobis (yiddol@mobis.co.kr)

Received: July 28, 2012; Accepted: March 11, 2013

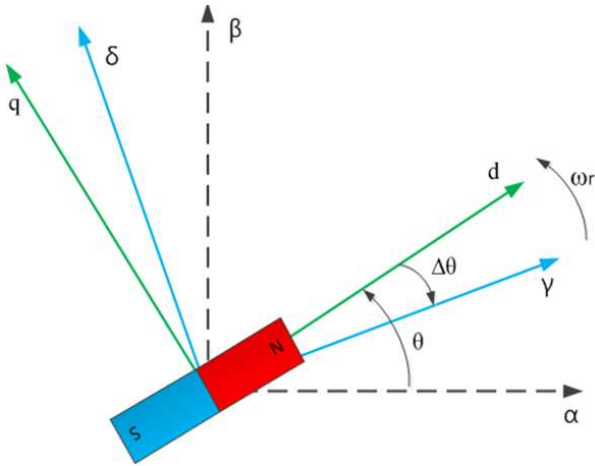


Fig. 1. Space vector diagram of IPMSM

axis which is synchronized with flux of real rotor. The estimated rotary coordinate axis without position sensor is γ - δ . The Fig. 1 also shows that there have error as much as $\Delta\theta$ between the two rotary coordinate axes.

Eq. (3) is obtained by changing the Eq. (2) with voltage equation on the estimated axis γ - δ of Fig. 1.

$$\begin{bmatrix} v_\gamma \\ v_\delta \end{bmatrix} = \begin{bmatrix} R+pL_d & p\Delta\theta L_d - \omega_r L_q \\ p\Delta\theta L_d + \omega_r L_q & R+pL_d \end{bmatrix} \begin{bmatrix} i_\gamma \\ i_\delta \end{bmatrix} + \begin{bmatrix} -E_x \sin \Delta\theta \\ E_x \cos \Delta\theta \end{bmatrix} \quad (3)$$

On the equation above, $p\Delta\theta$ which is the derivative of position error is too small value than ω_r at the steady state so that Eq. (4) below can be got by ignoring the derivative.

$$\begin{bmatrix} v_\gamma \\ v_\delta \end{bmatrix} = \begin{bmatrix} R+pL_d & -\omega_r L_q \\ \omega_r L_q & R+pL_d \end{bmatrix} \begin{bmatrix} i_\gamma \\ i_\delta \end{bmatrix} + \begin{bmatrix} -E_x \sin \Delta\theta \\ E_x \cos \Delta\theta \end{bmatrix} \quad (4)$$

If there is position error EMF is changed as like the extended EMF voltage equation of (4), $\Delta\theta$ can be seen through this EMF and Eq. (5) below.

$$\tan \Delta\theta = \frac{\sin \Delta\theta}{\cos \Delta\theta} \quad (5)$$

Making the Eq. (4) as a discrete equation for current, a model Eq. (6) can be defined as below.

$$\begin{bmatrix} i_{M\gamma}(n) \\ i_{M\delta}(n) \end{bmatrix} = \begin{bmatrix} 1 - \frac{R}{L_d} T & \omega_M \frac{L_q}{L_d} T \\ -\omega_M \frac{L_q}{L_d} T & 1 - \frac{R}{L_d} T \end{bmatrix} \begin{bmatrix} i_\gamma(n-1) \\ i_\delta(n-1) \end{bmatrix} + \frac{T}{L_d} \begin{bmatrix} v_\gamma(n-1) \\ v_\delta(n-1) \end{bmatrix} - \frac{T}{L_d} \begin{bmatrix} e_{xM\gamma} \\ e_{xM\delta} \end{bmatrix} \quad (6)$$

The current of motor which have position error $\Delta\theta$ can be expressed as Eq. (7) below.

$$\begin{bmatrix} i_\gamma(n) \\ i_\delta(n) \end{bmatrix} = \begin{bmatrix} 1 - \frac{R}{L_d} T & \omega_r \frac{L_q}{L_d} T \\ -\omega_r \frac{L_q}{L_d} T & 1 - \frac{R}{L_d} T \end{bmatrix} \begin{bmatrix} i_\gamma(n-1) \\ i_\delta(n-1) \end{bmatrix} + \frac{T}{L_d} \begin{bmatrix} v_\gamma(n-1) \\ v_\delta(n-1) \end{bmatrix} - \frac{T}{L_d} \begin{bmatrix} e_{x\gamma} \\ e_{x\delta} \end{bmatrix} \quad (7)$$

Calculating the error between model current of Eq. (6) and actual current, Eq. (8) can be obtained. However, the estimated speed and actual speed is equal ($\omega_r = \omega_M$) was assumed.

$$\begin{bmatrix} \Delta i_\gamma(n) \\ \Delta i_\delta(n) \end{bmatrix} = -\frac{T}{L_d} \begin{bmatrix} e_{x\gamma} - e_{xM\gamma} \\ e_{x\delta} - e_{xM\delta} \end{bmatrix} \quad (8)$$

Summarizing the Eq. (8) with respect to the error of Back-EMF, Eq. (9) can be obtained.

$$\Delta e_x = e_x - e_{xM}, \Delta e_x = -\frac{L_d}{T} \Delta i \quad (9)$$

Applying Eq. (9), a control equation such as Eq. (10) which can estimate the Extended EMV can be derived.

$$e_{xM}(n) = e_{xM}(n-1) - K_{ee} \Delta i(n) \quad (10)$$

The extended EMF is estimated as shown in Fig. 2 $\Delta\theta$ is obtained by using Eq. (11) from the estimated EMF, the speed and position are estimated using PI controller such as Eq. (11).

$$\omega_M(n) = \Delta\theta_e(n) \left(K_{P\omega} + \frac{K_{I\omega}}{s} \right) \quad \theta_M(n) = \int \omega_M(n) dt \quad (11)$$

$$\theta_M = \frac{K_{P\omega} s + K_{I\omega}}{s^2 + K_{P\omega} s + K_{I\omega}} \theta \quad K_{P\omega} = 2\zeta_n \omega_{no} \quad K_{I\omega} = \omega_{no}^2$$

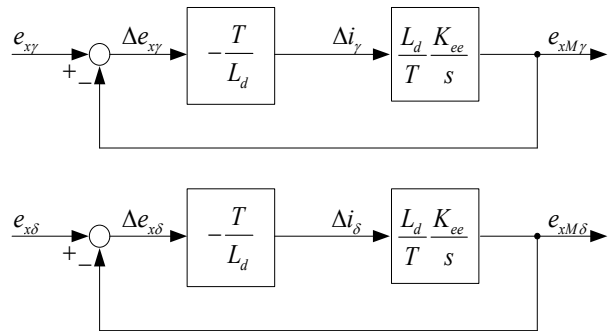


Fig. 2. Extended EMF estimation block diagram.

3. Sensorless Low Speed Region

It is difficult to estimate the exact position at extremely low speed region and stop which have not enough Back-EMF because extended EMF sensorless control method is a way that estimates positions by estimating Back-EMF. Therefore, It is required an algorithm doing sensorless control that can operate at extremely low speed region and stop in whole motor operating domain.

Eq. (13) can be obtained conversing with the value on the estimated axis using Eqs. (1) and (12). Eq. (14) can be seen summarizing the Eq. (13) for current. Eq. (14) is simplified as Eq. (15) assuming that neglecting resistor R and $\omega_r=0$ when injecting $V_{ac}\sin\omega_{ac}t$ which is enough fast sinusoidal voltage into the γ axis.

$$\begin{bmatrix} \gamma \\ \delta \end{bmatrix} = \begin{bmatrix} \cos \Delta\theta & \sin \Delta\theta \\ -\sin \Delta\theta & \cos \Delta\theta \end{bmatrix} \begin{bmatrix} d \\ q \end{bmatrix} \quad (12)$$

$$\begin{bmatrix} v_\gamma \\ v_\delta \end{bmatrix} = \begin{bmatrix} a_{11} & a_{12} \\ a_{21} & a_{22} \end{bmatrix} \begin{bmatrix} i_\gamma \\ i_\delta \end{bmatrix} + e \begin{bmatrix} -\sin \Delta\theta \\ \cos \Delta\theta \end{bmatrix}$$

$$\begin{aligned} a_{11} &= R + p(L_0 + L_2 \cos 2\Delta\theta) + \omega_r L_2 \sin 2\Delta\theta \\ a_{12} &= -pL_2 \sin 2\Delta\theta - \omega_r(L_0 - L_2 \cos 2\Delta\theta) \\ a_{21} &= -pL_2 \sin 2\Delta\theta + \omega_r(L_0 + L_2 \cos 2\Delta\theta) \\ a_{22} &= R + p(L_0 - L_2 \cos 2\Delta\theta) - \omega_r L_2 \sin 2\Delta\theta \end{aligned} \quad (13)$$

$$L_0 = \frac{L_d + L_q}{2} \quad L_2 = \frac{L_d - L_q}{2} \quad e = \omega_r K_E$$

$$p \begin{bmatrix} i_\gamma \\ i_\delta \end{bmatrix} = \frac{1}{L_0^2 - L_2^2} \begin{bmatrix} L_0 - L_2 \cos 2\Delta\theta & -L_2 \sin 2\Delta\theta \\ L_2 \sin 2\Delta\theta & L_0 + L_2 \cos 2\Delta\theta \end{bmatrix} * \quad (14)$$

$$* \left\{ \begin{bmatrix} v_\gamma \\ v_\delta \end{bmatrix} - \begin{bmatrix} R + \omega_r L_2 \sin 2\Delta\theta & -\omega_r(L_0 - L_2 \cos 2\Delta\theta) \\ \omega_r(L_0 + L_2 \cos 2\Delta\theta) & R - \omega_r L_2 \sin 2\Delta\theta \end{bmatrix} \begin{bmatrix} i_\gamma \\ i_\delta \end{bmatrix} - \omega_r K_E \begin{bmatrix} \sin \Delta\theta \\ \cos \Delta\theta \end{bmatrix} \right\}$$

$$p \begin{bmatrix} i_{\gamma ac} \\ i_{\delta ac} \end{bmatrix} = \frac{1}{L_0^2 - L_2^2} \begin{bmatrix} L_0 - L_2 \cos 2\Delta\theta \\ L_2 \sin 2\Delta\theta \end{bmatrix} V_{ac} \sin \omega_{ac} t \quad (15)$$

From the Eq. (15), the amplitude of ac current includes position error component. Therefore, it is possible to make the position error into zero and find the exact position of rotor by controlling the amplitude component of δ -axis ac current with zero, the amplitude of ac current $I_{\delta ac}$ can be obtained via FFT.[3] Thus speed and position can be estimated in the same way with Eq. (16).

$$I_{\delta ac} = FFT[i_\delta] = \frac{\omega_{ac}}{2\pi} \int_0^{2\pi} i_\delta \sin \omega_{ac} t dt \quad (16)$$

$$\omega_M(n) = I_{\delta ac} K_f \left(K_{p\omega} + \frac{K_{I\omega}}{s} \right) \quad \theta_M(n) = \theta_M(n-1) + T \omega_M(n-1)$$

At this, FFT can be obtained by moving average of one cycle because it knows the frequency for AC input. In this way, the 180° error may be included in some cases because

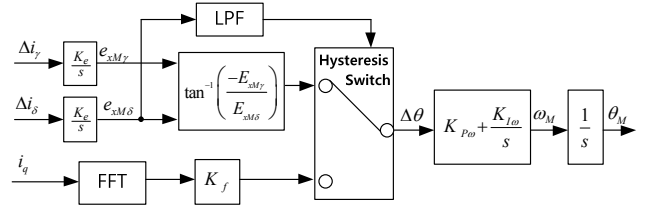


Fig. 3. Conversion of Sensorless Method block diagram.

it uses $2\Delta\theta$ as the above equation when stop. Magnetic pole should be decided after finished the estimation of stop position because 180° error is existed between N and S pole. Eq. (15) becomes Eq. (17) after finishing the initial position estimation.

$$p \begin{bmatrix} i_{\gamma ac} \\ i_{\delta ac} \end{bmatrix} = \begin{bmatrix} 1 \\ L_d \\ 0 \end{bmatrix} V_{ac} \sin \omega_{ac} t \Rightarrow p i_{\gamma ac} = \frac{V_{ac}}{L_d} \sin \omega_{ac} t \quad (17)$$

That is, only the current of γ axis is left but amplitude of AC is increased rapidly because there is inductance L_d which is reduced if there happens saturation flux on the denominator of amplitude. Therefore, when AC voltage which is enough to saturate magnetic flux is applied, it is the estimated stop position if the positive AC is increased high, but there is 180° error if negative AC is increased to compensate it. Finally, the exact stop position estimation is possible by using these methods.

It is very important that combine the two methods because there have differences between sensorless control in low speed and middle-high speed mode. In this paper, we built a diagram to shift the sensorless control in low and middle-high speed as shown in Fig. 3 Low speed and middle-high speed region are classified by applying the estimated δ -axis EMF through low pass filter. In case that δ -axis EMF is small, $\Delta\theta$ which is estimated from the low speed region sensorless control was used. On the contrary, $\Delta\theta$ is estimated from the extended EMF model in the case of large δ -axis EMF. It is required that hysteresis to prevent the frequent shift of the two methods.

4. Sensor Failure Detection

Hybrid cars are basically equipped with position sensor. So, normally they do not require position sensorless drive. But to prepare for position sensor failures, it is necessary to locate sensorless algorithm driving even while position sensor driving is on operation. [4] However, in case the sensorless algorithm operates when driving the position sensor, the estimated location and speed will not be used on either side so it be open loop condition that speed ω_M and location θ_M are diverged. Therefore, if input on the sensorless algorithm the conversed values for the voltage and current of the actual IPM to get the feedback of

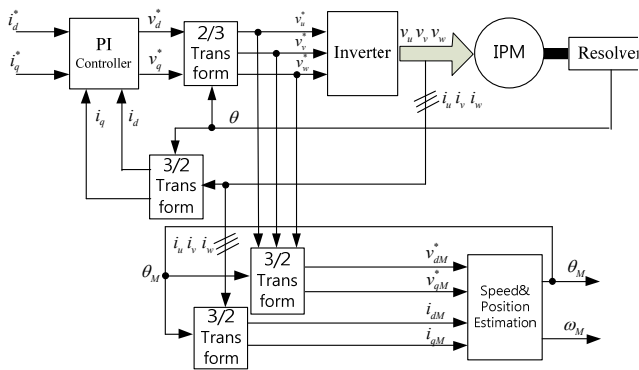


Fig. 4. Proposed control Method

estimated location, it operates independently without diverging for the estimated speed and location so that it can be used whenever it is required instead of position sensor. Fig. 4 shows block diagram of sensorless control under the driving of position sensor. As seen on the Fig. 4, current control is executed using rotor location information θ while motor is driving. In parallel, sensorless algorithm also estimates θ_M as described before. If the error between θ and θ_M surpasses the allowable range, it can be regarded as the failure of position sensor and the motor should be controlled with θ_M .

5. Result of experiments

Experiments are executed to verify the effectiveness of the proposed methods. Fig. 5 are the motor and inverter which are used in the experiments. The motor is 15kW IPMSM and driving voltage is DC 150V.

Fig. 6 shows that estimating initial location by using proposed low speed region sensorless method. It can verify through waveform that there having different locations for actual and estimated at beginning but the estimated is followed the actual location at the same time of use estimating algorithm.



Fig. 5. Motor & Inverter used in the experiment.

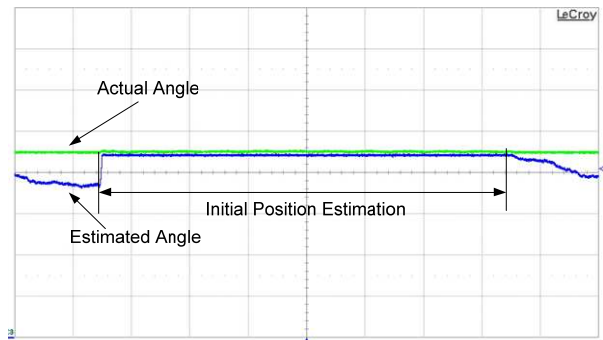


Fig. 6. Initial location estimation when stop.

Figs. 7 and 8 are the waveform that showing initial location estimation when stop and pole decision. Top of the Figure is actual angle and estimated one and the bottom of the Figure is the phase current of motor. The voltage harmonics applied to estimate the initial position so that phase currents alternate with the frequency of voltage harmonic. The pole decision is executed after initial position is estimated. In case of Fig. 7, actual angle is match with estimated one it can be verified the size of positive phase current increase. In case of Fig. 8, it has 180° error between actual and estimated angle and can verify that the wave of phase current increase for the negative direction. Comparing the maximum value of the

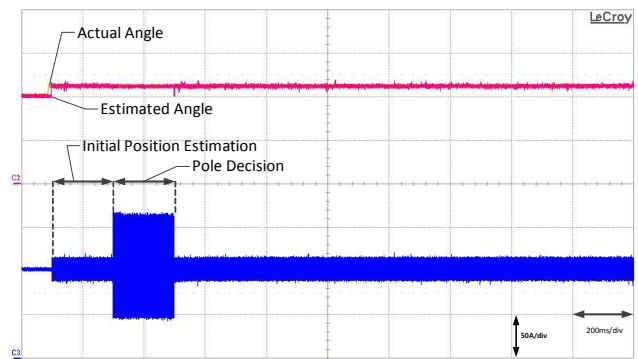


Fig. 7. Initial location estimation when stop without 180° error .

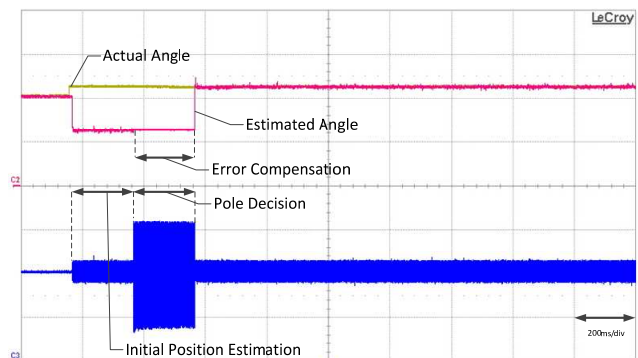


Fig. 8. Initial location estimation when stop with 180° error .

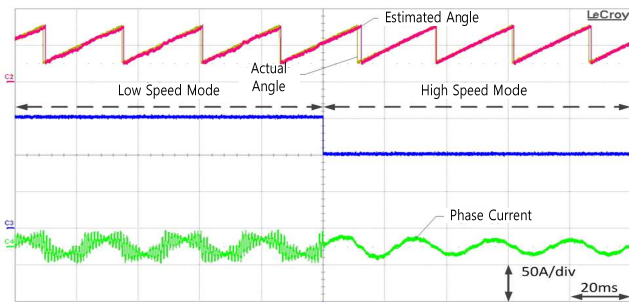


Fig. 9 Shift from Low speed to High speed.

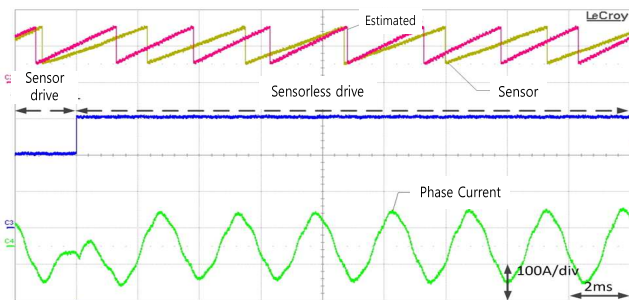


Fig. 10 Fault detection and sensorless shift.

positive and negative current, in the case that increasing for positive accept the initial estimated position as itself and compensated with 180° when increase for negative.

Fig. 9 shows the waveform that driving with the low-speed algorithm then switches with middle-high speed algorithm. Top waveform of the picture is actual and estimated angle, middle waveform is for distinguish low and high speed and the bottom is for phase current of the motor. Algorithm is shifted at the 300RPM driving start with low speed mode algorithm. Phase current includes the current affected by harmonic which is applied in low speed mode but can also see the waveform which is removed harmonic by shifting with high speed mode harmonic is not applied.

It can verify through waveform that the algorithm shifts without any problem. As see the estimated waveform, it has more large error with the actual angle in the low speed mode. The judgment of low speed and high speed mode is executed by using the size of EMF which is estimating in the sensorless algorithm.

Fig. 10 is the waveform that is shifted with sensorless after sensor failure under operating at the rated load and 3000RPM. Sensor failure is implemented by separating the signal line of Resolver with the controller under normal operation applied sensor. It programmed that if the error of actual and estimated angle is over 40° shift with sensorless mode after sensor failure. Even though the line of sensor is open, actual angle is not stopped immediately and keeps coming out with incorrect values and stop. The speed of stopping an actual angle after signal line is opened is shown faster, as the rotation speed becomes slower. We

concluded that this situation is from Resolver customized IC we used and the IC has some compensation algorithm. In the waveform of phase current, the current control is not performed normally at right before shift from sensor mode to sensorless mode due to the large error between actual rotor and Resolver location but showed that it is controlled normally after shift with sensorless.

6. Conclusion

In this paper, the sensorless algorithm and sensor failure detection method for sensorless operation when the position sensor of IPMSM is failed are proposed. Two sensorless algorithms are implemented for low-speed and middle-high speed. Middle-high speed algorithm that can estimate back-EMF with relatively simple than the exist algorithm was proposed. In low-speed algorithm, a method which compensate the disadvantage which can happen existed 180° error with the pole decision was proposed. The proposed methods were verified through experiments for its effectiveness. In future, reliability verification tests and additional researches about how quickly and accurately the sensor failure can be determined and shifted for practical applications will be proceed.

Acknowledgements

This work was supported by Hyundai Mobis Company.

References

- [1] Shigeo Morimoto, Keisuke Kawamoto, Masayuki Sanada, and Yoji Takeda, "Sensorless Control Strategy for Salient-Pole PMSM Based on Extended EMF in Rotating Reference Frame," *IEEE Trans. Ind. App.*, vol. 38, no.4, pp.1054-1061, July/Aug. 2002.
- [2] Z. Chen, M. Tomita, S. Ichikawa, S. Doki, and S. Okuma, "Sensorless control of interior permanent magnet synchronous motor by estimation of an extended electromotive force," in *Conf. Rec. IEEE-IAS Annul Meeting, 2000*, pp. 1814-1819.
- [3] T. Aihara, T. Yamase "Sensor-less Torque Control of Salient-Pole Synchronous Motor at Zero Speed Operation", 1997, *JIASC'97*, 170.
- [4] K.W Lee, "Position Sensor Fault Tolerant Control of Permanent Magnet Synchronous Generator," *KIPE, KIPE Trans, Vol.15 No.4 2011.8*, page(s): 351-357.
- [5] S.T LEE, J.H Cho, D.G Kim, "Trends in the development of electric vehicle drive system," *KIPE, KIPE JOURNAL VOL.16 No.2, 2011.4*, page(s): 22-78.



Sung-Joo Kim He was born in Seoul, Korea in 1982. He received his B.S. in Electronic Engineering from Cheongju University, Cheongju, Korea, in 2008. From 2007 to 2010, he was a Researcher with the Ewha Technologies information R&D Center, Gwangju, Korea. He is currently M.S Candidate in Dept. of Electrical Engineering, Konkuk University, Seoul, Korea. His research interests include sensorless drive of ac drive, Parameter estimation drive of Induction Motor.



Yong-Kyun Lee He was born in Seoul, Korea in 1977. He received his B.S., M.S. and Ph.D. in Electrical Engineering from Konkuk University, Seoul, Korea, in 2001, 2005 and 2013, respectively. Since 2005, he has been a Research Engineer with the Technical Research Institute at Vtech.



Ju-Suk Lee He received the B.S degree in electrical engineering from Korea University, Seoul, Korea, in 1993, the M.S. and the Ph.D. degrees in electrical engineering from Nagoya Institute of Technology, Nagoya, Japan in 1998, 2000, respectively. From 2000 to 2002 he was a Research Engineer with Technology Research Center of Sumitomo Heavy Industries, Yokosuka, Japan. He is currently an Assistant Professor in Dept. of Mechanical Air-Conditioning, Gyeonggi College of Science and Technology, Siheung, Korea. His research interests include sensorless drive of ac drive, flux –weakening control and DTC drive of PMSM.



Kwang-Woon Lee He received his B.S., M.S., and Ph.D. in Electrical Engineering from Korea University, Seoul, Korea, in 1993, 1995, and 1999, respectively. From 2000 to 2002, he was with Samsung Advanced Institute of Technology, Yongin, Korea, where he worked on the development of micro-electromechanical system sensor applications. From 2002 to 2007, he was a Senior Research Engineer with the Samsung Living Appliance R&D Center, Samsung Electronics, Suwon, Korea, where he was engaged in research on sensorless motor drive systems for refrigerators and air conditioners. He is currently an Assistant Professor in the Department of Electronic Engineering, Mokpo

National Maritime University, Mokpo, Korea. His current research interests include power electronics and control, which include ac machine drives, digital-signal-processing-based control applications, and fault diagnosis of electrical machines.



Taesuk, Kwon He received B.S. and M.S. degrees in electrical engineering from Hanyang University, Seoul, Korea, in 1995 and 1997, respectively, and Ph.D. degree in electrical engineering from Seoul National University, Seoul, Korea in 2007. From 1997 to 2003, he was a Research engineer with Hyundai Elevator Company, Ichon, Korea, where he developed high speed gearless elevator systems. Since 2008, he has been a Principal Research engineer with Hyundai Mobis Company, Yongin, Korea, where he is currently researching on a subject about power electronics component for a xEV application. His research interests include high performance ac drives, power converters, and electric drive systems for xEVs.



Hyungsoo Mok He received the B.S., M.S. and Ph.D. degrees in electrical engineering from Seoul National University, Korea, in 1986, 1988, and 1992, respectively. He was with the Department of Control and Instrumentation Engineering at Seoul National Polytechnic University from 1993 to 1997. Since 1997, he has been with the Department of Electrical Engineering at Konkuk University. His teaching and research interests include electric machines, electric machine drive systems, and power electronic control for industrial and power systems.